Radiation Conductance and Pattern of Array Antenna on a Non-Confocal Dielectric-Coated Elliptic Cylinder

A. HELALY* and A. SEBAK
Electrical and Computer Engineering Dept
Concordia University
Montreal, QC, H3G 1M8, CANADA
* Engineering Mathematics and Physics Dept, Cairo University, Giza, EGYPT
aahelaly@yahoo.com http://eng.cu.edu.eg, abdo@ece.concordia.ca http://encs.concordia.ca

Abstract- The formulation for the radiation pattern and conductance of axial slots array antenna on a dielectric-coated elliptic cylinder is presented. The coating is assumed to be non-confocal. The analytical solution, given here, is based on the eigen function technique and the addition theorem of Mathieu functions. The excited apertures are assumed to generate a TM polarized wave. Accordingly, the obtained series solution is truncated to generate numerical results. Sample of calculated azimuthal radiation patterns and radiation conductance are presented for different antenna and coating parameters. The elliptic cylinder has one extra degree of freedom compared to a circular cylinder to control the radiation pattern and conductance. The computed results show the flexibility of the antenna to control the shape and direction of its radiation pattern by changing the frequency, the excitation, the coating thickness of the cylinder, and the constitutive parameters of the coating.

Key-Words: Axial slot antennas, non-confocal coating, analytical methods.

1. Introduction

Arrays of antennas mounted on vertical structures are useful for the broadcasting of waves and for base stations [1-3]. Many such geometrical structures have been analytically treated. The axial and circumferential slots on circular and elliptical cross-sectional conducting cylinders were treated in [4-6]. The dielectric-coated circulars or elliptical cross-sectional conducting cylinders were considered in [7-13]. The elliptic geometry is becoming more popular since it allows a better control of the polarization characteristics and facilitates the design by changing both eccentricity and focal length to tune the parameters of interest. In addition, the non-uniform coating offers another degree of design freedom. Also, elliptic cylindrical cavities excite more propagating modes compared to circular cavities [14]. For the analysis of such antennas, the homogeneous Helmholtz equation in the elliptic coordinates is employed. Solving field problems of structures with elliptical geometries requires the computation of Mathieu and modified Mathieu functions [15]. These are the eigen solutions of the wave equation in elliptical coordinates. The analytical developments of the solution for far field patterns of the multi-slotted elliptic cylinder with concentric coating have been presented in [12].

The studies presented in this paper are focused on the analysis and design of a finite array of axial slots on a non-confocal dielectric-coated conducting elliptic cylinder. The work is an extension of the formulation for a single slot antenna on an elliptic cylinder [11]. One of the motivations for this work is to study the effect of a dielectric layer on the performance of antennas mounted on a space shuttle. We assumed that the aperture field i.e., the excitation voltages, is a specified function on each slot. The fields in the dielectric coating and exterior regions are expanded in terms of Mathieu and modified Mathieu functions with unknown expansion coefficients. These unknown expansion coefficients are determined by enforcing appropriate boundary conditions at the interface between the dielectric coating and free space and at the slotted cylinder. In order to generate numerical results and from a practical point of view, the series solution must be truncated in a suitable fashion to obtain a finite

size matrix. The order of such a matrix depends on the electrical size and properties of the coating region.

2. Problem Formulation

The configuration of the axial array antenna mounted on elliptic cylinder is shown in Fig. 1. The antenna radiates through a non-confocal dielectric coating (region II) to free space (region I). Two systems of coordinates are used. The global coordinates at the center of the outer surface of the dielectric coating are identified by (x, y). The local coordinates at the center of the slotted conducting cylinder are (x_c, y_c). The semi major and semi minor axes for the conducting cylinder are denoted by a_c and b_c. The corresponding parameters for the coating region are a and b. The focal length of the dielectric outer surface is 2F and that of the conducting cylinder is denoted by $2F_c$. The major axis of the cross section of the conducting cylinder is inclined by an angle β with respect to the x axis and its center is located at (d, ψ) with respect to the global coordinates. The elliptical coordinates (u, v, z) are employed throughout with x = F cosh (u) cos (v) and y = F sinh (u) sin (v) where F is the semi focal length of the corresponding elliptical cross section.

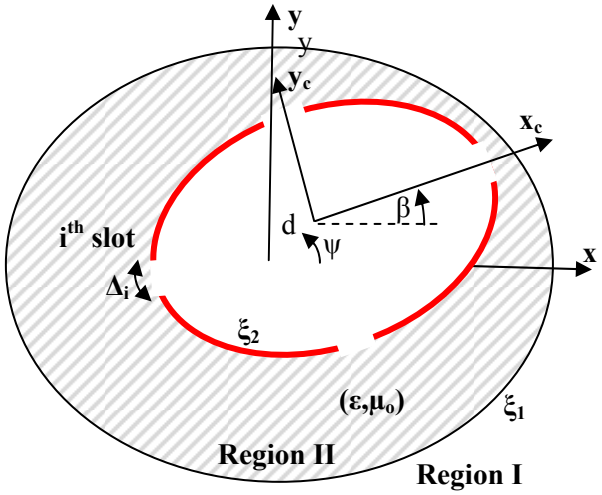

Fig. 1: Configuration of axial slotted-elliptic cylinder array antenna coated with a non-confocal dielectric.

This paper considers the TM polarization in which the non zero field components are E_z, H_ρ and H_φ. It is assumed that the filed distribution on the slots depends on the angular variable v. In region I and using the global coordinates (u, v), the electric field component is given by

$$E_z^{(I)} = \sum_{m=0}^{\infty} Be_m \,\mathrm{Re}_m^{(4)}(c_0,\xi) Se_m(c_0,\eta) + \sum_{m=1}^{\infty} Bo_m Ro_m^{(4)}(c_0,\xi) So_m(c_0,\eta) \quad (1)$$

where ξ = cosh (u), η = cos (v) and $c_0 = k_0 F, k_0 = 2\pi/\lambda$ and λ is the free space wavelength. Se_m, So_m are, respectively, the even and odd angular Mathieu functions of order *m*, $\mathrm{Re}_m^{(4)}$, $Ro_m^{(4)}$ are the even and odd modified Mathieu functions of fourth kind. The corresponding magnetic field components are given by

$$H_\eta = \frac{-j}{2\omega\mu_o h}\frac{\partial E_z}{\partial \xi} \quad (2a)$$

$$H_\xi = \frac{-j}{2\omega\mu_o h}\frac{\partial E_z}{\partial \xi} \quad (2b)$$

where $h = F\sqrt{\dfrac{\xi^2-1}{\xi^2-\eta^2}}$

The electric field component in region II must vanish on the conducting part of the core cylinder except at the slots. In region II and using the local coordinates, we may express it in the form

$$E_z^{(II)} = \sum_{m=0}^{\infty} \left(\begin{bmatrix} Ce_m \,\mathrm{Re}_m^{(1)}(c_3,\xi_c) \\ + De_m \,\mathrm{Re}_m^{(2)}(c_3,\xi_c) \end{bmatrix} Se_m(c_3,\eta_c) + \begin{bmatrix} Co_m Ro_m^{(1)}(c_3,\xi_c) \\ + Do_m Ro_m^{(2)}(c_3,\xi_c) \end{bmatrix} So_m(c_3,\eta_c) \right) \quad (3)$$

where ξ_c = cosh (u_c), η_c = cos (v_c) and $c_3 = kF_c$ with $k = k_o\sqrt{\varepsilon_r}$. $\mathrm{Re}_m^{(i)}$, $Ro_m^{(i)}$ are the even and odd

modified Mathieu functions of the ℓ^{th} kind. The corresponding magnetic field components are given by (2) but using the local coordinates. In (1) and (3) B, C and D are unknown expansion coefficients to be determine by enforcing proper boundary conditions on the antenna and the interface between the dielectric and free space.

2.1 Boundary Conditions

The three sets of unknown expansion coefficients are determined by applying boundary conditions on the two surfaces: the core conducting cylinder and the interface between the coating material and free space.

2.1.1 Core (antenna) boundary

On the conducting surface $\xi = \xi_2$, the tangential electric field component must vanish except on the slots. Using the local coordinates, the boundary condition may be expressed as:

$$E_z^{(II)} = \begin{cases} F(\eta_c) & \text{on the slots} \\ 0 & \text{otherwise} \end{cases} \qquad (4)$$

Where

$$F(\eta_c) = \sum_{i=1}^{N} F_i(\eta_c) \qquad (5)$$

is the aperture field distribution on the slots.

On the i^{th} slot, it is assumed that the excitation voltage is varying as

$$F_i(\eta_c) = V_i e^{j\delta_i} \cos(\pi(v_c - v_{oi})/2\Delta_i), \qquad (6)$$

$V_i e^{j\delta_i}$ is the applied voltage, v_{oi} is the angular coordinate of its center, Δ_i is its width and $\eta_c = \cos(v_c)$ in the (x_c, y_c) local coordinates. Substituting (3) and (5) in (4), multiplying the results by $S_{\substack{e\\o}n}(c_3, \eta_c)$ and applying the orthogonality of Mathieu functions [16], the terms involving even functions decouple completely from those of odd functions. Thus, one obtains two subsystems of linear equations for the even and odd unknown expansion coefficients. For the even functions the resulting subsystem of equation is given by, n = 0, 1, 2, ….,

$$N_{e_n}(c_3)[Ce_n \,\mathrm{Re}_n^{(1)}(c_3, \xi_2) + De_n \,\mathrm{Re}_n^{(2)}(c_1, \xi_2)] = \int_{slots} F(\eta_c) Se_n(c_3, \eta_c) d\eta_c = F_e(c_3) \qquad (7)$$

For the odd functions case and for n = 1, 2, 3, …

$$N_{o_n}(c_3)[Co_n Ro_n^{(1)}(c_3, \xi_2) + Do_n Ro_n^{(2)}(c_1, \xi_2)] = \int_{slots} F(\eta_c) So_n(c_3, \eta_c) d\eta_c = F_o(c_3) \qquad (8)$$

Ne_n, No_n are normalized constants and given by [12];

$$N_{\substack{e\\o}n}(c_3) = \int_0^{2\pi} [S_{\substack{e\\o}n}(c_3, \eta)]^2 dv, \qquad \eta = \cos v \qquad (9)$$

And Fe, Fo are the slots excitation vector and given by;

$$F_{\substack{e\\o}n}(c_3) = \sum_{i=1}^{N} \int_{i^{th}slot} F_i(\eta) S_{\substack{e\\o}n}(c_3, \eta) dv \qquad (10)$$

2.2.2 Coating – fre space boundary

On the outer surface of the dielectric coating, i.e., $\xi = \xi_1$, the continuity of both E and H field tangential components must be enforced. The field components inside the coating region can be expressed in terms of the global coordinate system using the transition theorem of Mathieu functions [17], see the Appendix. Again using the orthogonal properties of Mathieu functions, one obtains from the tangential E_z filed component:

$$\sum_{m=0}^{\infty} Me_{nm}(c_3,c_0)Be_m \,\mathrm{Re}_m^{(4)}(c_0,\xi_1) =$$
$$Ne_n(c_3)\,\mathrm{Re}_n^{(1)}(c_3,\xi_1)\bullet$$
$$[\sum_{m=0}^{\infty} WEe_{nm}Ce_m + \sum_{m=1}^{\infty} WEo_{nm}Co_m]$$
$$+ Ne_n(c_3)\,\mathrm{Re}_n^{(2)}(c_3,\xi_1)\bullet$$
$$[\sum_{m=0}^{\infty} WEe_{nm}De_m + \sum_{m=1}^{\infty} WEo_{nm}Do_m] \quad (11)$$

And from the tangential H_v filed component, we obtain:

$$\frac{\mu_1}{\mu_0}\sum_{m=0}^{\infty} Me_{nm}(c_3,c_0)Be_m \,\mathrm{Re}_m^{(4)}{}'(c_0,\xi_1)$$
$$= Ne_n(c_3)\,\mathrm{Re}_n^{(1)}{}'(c_3,\xi_1)\bullet$$
$$[\sum_{m=0}^{\infty} WEe_{nm}Ce_m + \sum_{m=1}^{\infty} WEo_{nm}Co_m]$$
$$+ Ne_n(c_3)\,\mathrm{Re}_n^{(2)}{}'(c_3,\xi_1)\bullet$$
$$[\sum_{m=0}^{\infty} WEe_{nm}De_m + \sum_{m=1}^{\infty} WEo_{nm}Do_m] \quad (12)$$

$$\sum_{m=0}^{\infty} Mo_{nm}(c_3,c_0)[Bo_m Ro_m^{(4)}(c_0,\xi_1)]$$
$$= No_n(c_3)\,\mathrm{Re}_n^{(1)}(c_3,\xi_1)\bullet$$
$$[\sum_{m=0}^{\infty} WOe_{nm}Ce_m + \sum_{m=1}^{\infty} WOo_{nm}Co_m]$$
$$+ No_n(c_3)Ro_n^{(2)}(c_3,\xi_1)\bullet$$
$$[\sum_{m=0}^{\infty} WOe_{nm}De_m + \sum_{m=1}^{\infty} WOo_{nm}Do_m] \quad (13)$$

$$\frac{\mu_1}{\mu_0}\sum_{m=0}^{\infty} Mo_{nm}(c_1,c_0)[Bo_m Ro_m^{(4)}{}'(c_0,\xi_1)]$$
$$= No_n(c_1)Ro_n^{(1)}{}'(c_1,\xi_1)\bullet$$
$$[\sum_{m=0}^{\infty} WOe_{nm}Ce_m + \sum_{m=1}^{\infty} WOo_{nm}Co_m]$$
$$+ No_n(c_1)Ro_n^{(2)}{}'(c_1,\xi_1)\bullet$$
$$[\sum_{m=0}^{\infty} WOe_{nm}Ce_m + \sum_{m=1}^{\infty} WOo_{nm}Co_m] \quad (14)$$

Where $c_1 = k_1 F$, the prime denotes derivative with respect to ξ and

$$M_{\substack{e\\o}mn}(c_i,c_j) = \int_0^{2\pi} S_{\substack{e\\o}n}(c_i,\eta)S_{\substack{e\\o}m}(c_j,\eta)dv\,, \quad (15)$$

Equations (7)-(8) and (11–14) constitute a system of linear equations of unknown expansion coefficients of the fields: namely: $Be_m, Bo_m, Ce_m,$ Co_m, De_m and Do_m. Expressions for the transformation coefficients $WE_{\substack{e\\o}nm}$ and $WO_{\substack{e\\o}nm}$ are given in the appendix.

3 Radiated Power Density

Employing the asymptotic expansion of $\mathrm{Re}_m^{(4)}$ and $Ro_m^{(4)}$ in equation (1), the far radiated field, which is of particular interest, is given by;

$$E_z = \sqrt{j/(k\rho)}\; e^{-jk\rho}\sum_m j^m [Be_m Se_m(c_0,\eta) + Bo_m So_m(c_0,\eta)] \quad (16)$$

The time-average power density radiated by the antenna is then given by:

$$P(\rho,\phi)=\frac{1}{120\pi\, k\rho}\left[\sum_m j^m[Be_m Se_m(c_0,\cos\phi) + Bo_m So_m(c_0,\cos\phi)]\right]^2 \quad (17)$$

The average power density is defined as

$$P_{av}(\rho)=\frac{1}{2\pi}\int_0^{2\pi} \mathrm{P}(\rho,\phi)\mathrm{d}\phi \quad (18)$$

The antenna directivity is then given by

$$D(\rho,\phi)=\frac{P(\rho,\phi)}{P_{av}(\phi)} \quad (19)$$

For a single slot antenna, we define the radiation conductance per unit length as

$$G=2\pi\rho\frac{P_{av}(\phi)}{|V_o|^2} \quad (20)$$

Where V_o is the slot voltage.

4 Numerical Results

For illustration purposes, we consider the case of two slots each with width $\Delta=2^o$. For all considered cases, the electrical and geometrical parameters are given in each figure caption. Fig. 2 shows the radiation pattern for a single slot case and when the two slots are on the minor axis of the conducting cylinder. The pattern is similar to that of a pair of dipoles. The effect of location of the slots pair on the pattern is shown in Fig.3. For this case the outer boundary of the coating dielectric is of circular shape. Fig. 4 represents the effect of the excitation phase on the radiation pattern. It is seen that the main beam direction is steered 90^o when the phase is switched from the in-phase status to out of phase condition. Figure 5 shows the radiation patterns for an axially slotted elliptic cylinder with no coating but with in-phase excitation. The effect of the location of the two slots on the radiation patterns for an axially slotted elliptic cylinder is shown in Fig. 6. In Fig. 7, we compare the effect of the core shape on the radiation patterns for an axially slotted circular and elliptical one both coated with the same material. Figure 8 shows the radiation patterns for an axially slotted elliptic cylinder coated with a dielectric for two types of excitation: in-phase and out of phase.

Finally, we investigate the effect of different design parameters on the radiation conductance of s single slot antenna. In the following two figures Δ/λ represents the electrical thickness of the coating. Figure 9 shows that the radiation conductance depends on the coating material and its thickness. The effect of the slot location is demonstrated in Fig. 10 where the two cases considered are when the slot is located at the end of the major and minor axes. It is very clear from Figs. 9 and 10 that the radiation conductance depends strongly on the coating parameters: dielectric type, thickness of the coating and its shape.

5 Conclusion

An analytic solution is given for the radiation by an array of axial slots mounted on a conducting elliptic cylinder coated with a non-confocal dielectric. Results are presented for both the radiation pattern and radiation conductance for several geometrical and material parameters. The computed results show the flexibility of the antenna to control the shape and direction of its radiation pattern.

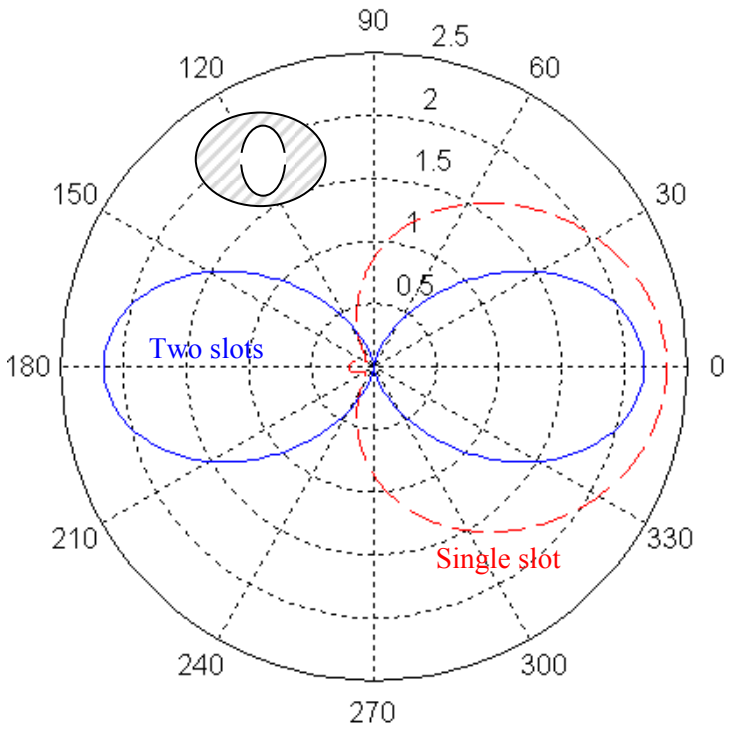

Fig 2: Radiation pattern for an axially slotted elliptic cylinder (a_c=0.15λ, a_c/b_c=2) coated with a dielectric (ε_r=4, a =0.4λ, a /b=2, d=0, ψ=0, β=90^o). The *two* out of phase slots with equal amplitude are located at the ends of the minor axis.

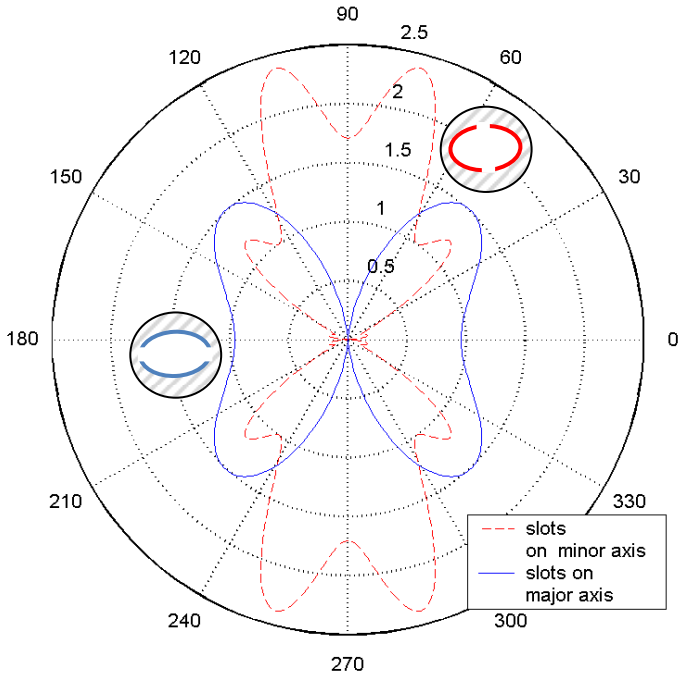

Fig. 3: Radiation pattern for an axially slotted elliptic cylinder (a_c=0.25λ, a_c/b_c=2) coated with a circular dielectric (ε_r=4, a=b=0.3λ, d=0, ψ=0, β=0). The *two* slots are fed with out of phase equal amplitude voltages: effect of the slots locations.

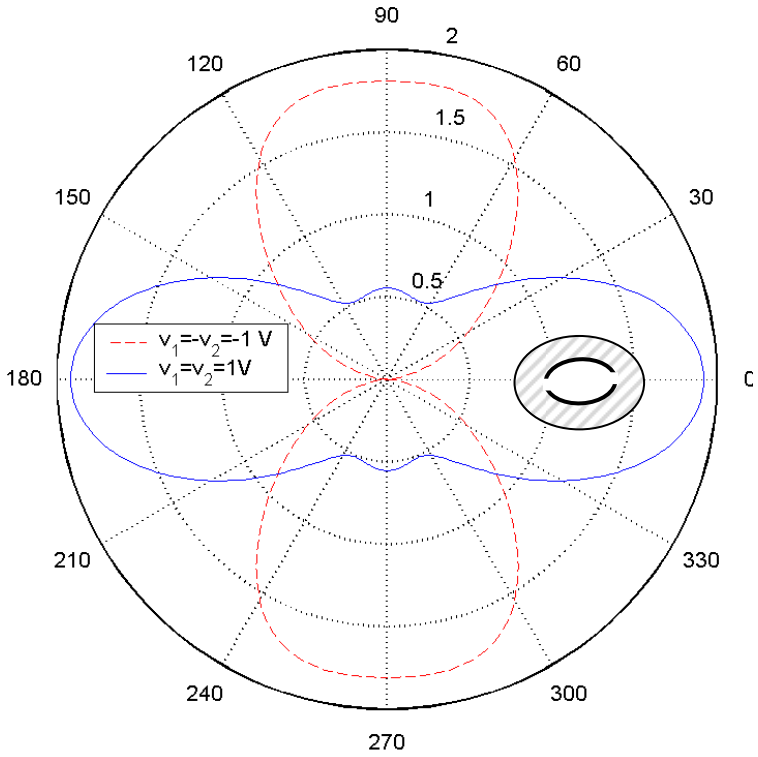

Fig. 4: Radiation patterns for an axially slotted elliptic cylinder (a_c=0.25λ, a_c/b_c=2) coated with a dielectric (ε_r=4, a=0.3λ, a /b=2, d=0, ψ=0, β=0). The *two* slots are located at the ends of the major axis: in-phase and out of phase excitation comparison.

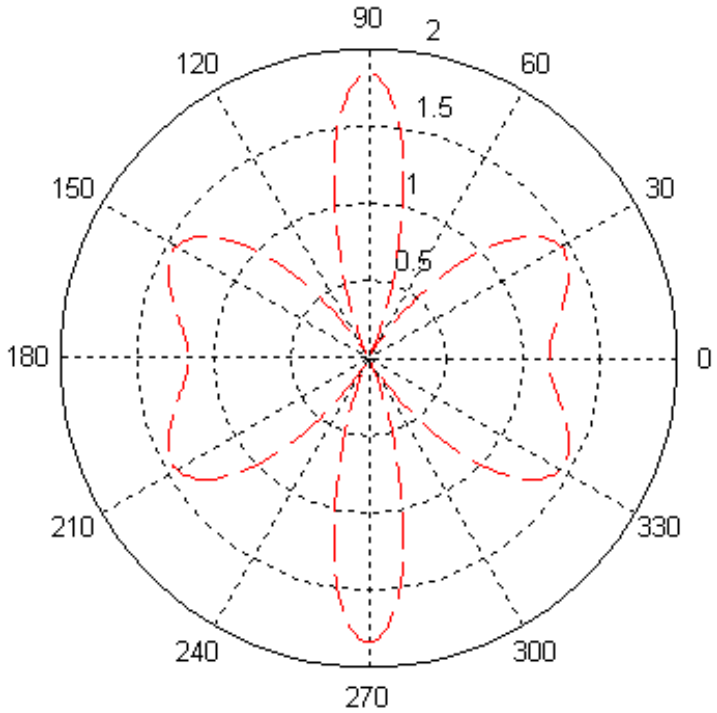

Fig. 5 Radiation patterns for an axially slotted elliptic cylinder (a_c=0.5λ, a_c/b_c=2) with no coating. The *two* slots are located at the ends of the major axis with in-phase excitation.

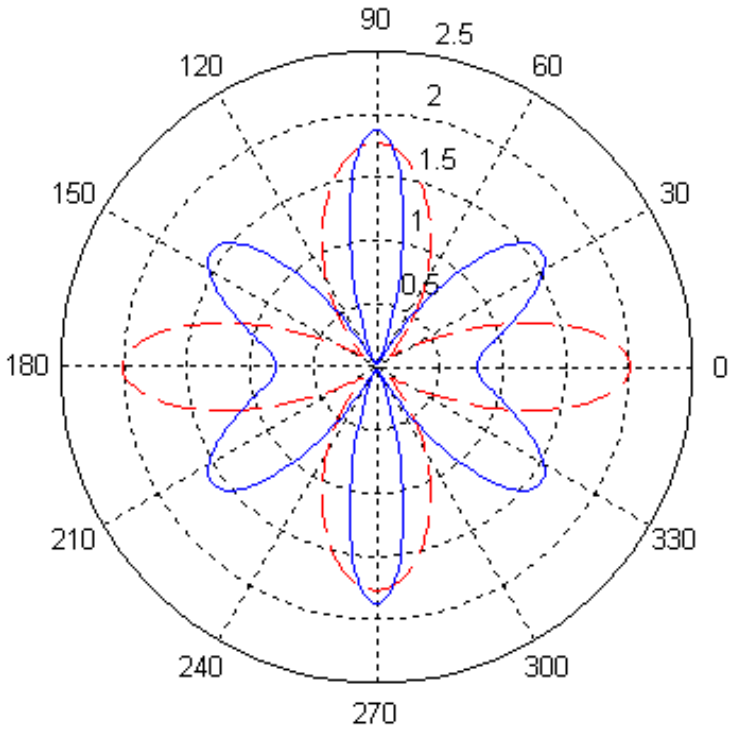

Fig. 6: Radiation patterns for an axially slotted elliptic cylinder (a_c=0.5λ, a_c/b_c=2)) coated with a dielectric (ε_r=4, a=0.6λ, a /b=2, d=0, ψ=0). The *two* in-phase slots are located at the ends of the major axis (solid line) and at the ends of minor axis (dashed line).

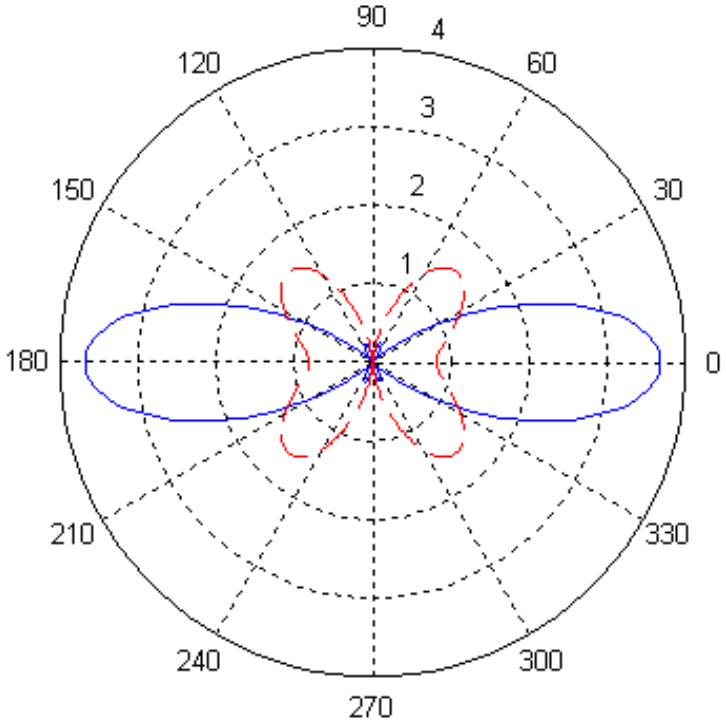

Fig. 7: Radiation patterns for an axially slotted circular (a_c=0.25λ, a_c/b_c=1: red dashed line) and elliptical (a_c=0.25λ, a_c/b_c=2: solid blue line) cylinder coated with a dielectric (ε_r=4, a=0.6λ, a /b=2, d=0, ψ=90^o). The *two* out of phase slots are located at the ends of the minor axis major axis (solid line) and at the ends of minor axis (dashed line).

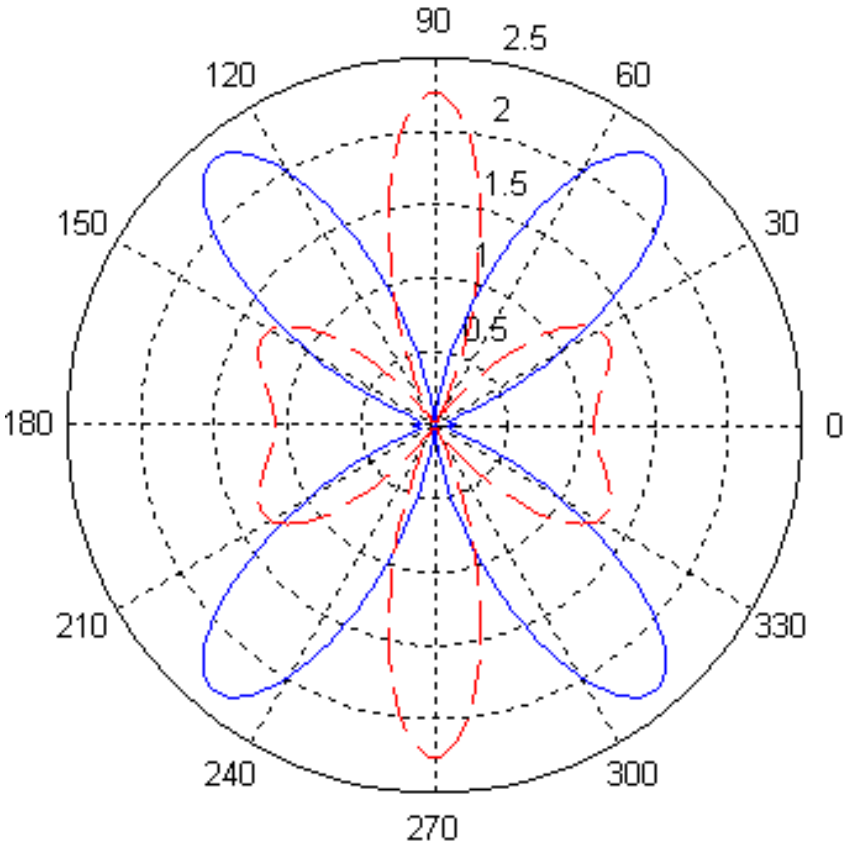

Fig. 8: Radiation patterns for an axially slotted elliptic cylinder (a_c=0.125λ, a_c/b_c=2) coated with a dielectric (ε_r=4, a=0.6λ, a /b=2, d=0, ψ=0, β=0). The *two* slots are located at the ends of the major axis: in-phase (solid blue line) and out of phase (dashed red line) excitation comparison.

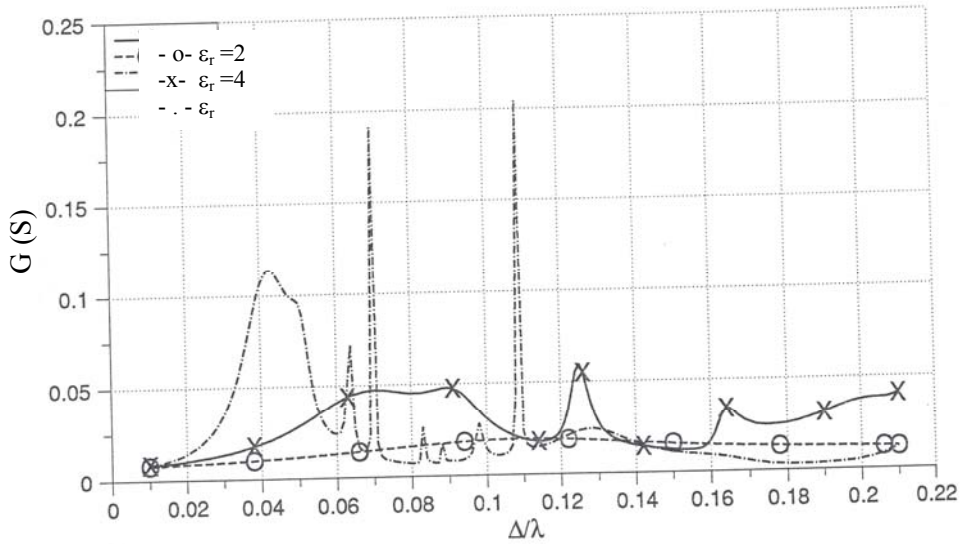

Fig. 9: Effect of coating material and thickness on the radiation conductance (a_c=0.25λ, $a/b=a_c/b_c$=2, $a=a_c+\Delta$, d=0, ψ=0, β=0). The slot is located at the end of the major axis.

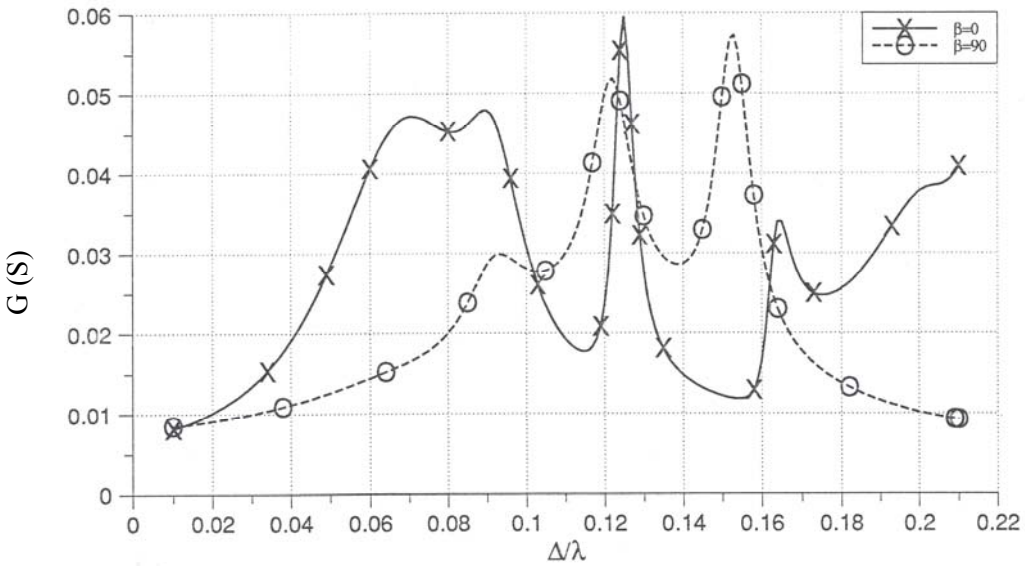

Fig. 10: Effect of slot location on the radiation conductance (a_c=0.5λ, a_c/b_c=2, $a/b=a_c/b_c$=2, $a=a_c+\Delta$, d=0, ψ=0, β=0). The slot is located at the end of the major axis (xx) and minor axis (oo).

Appendix

Consider two elliptic coordinate systems: (ξ_r,η_r,z) and (ξ_q,η_q,z). Outside the region which is bounded by the circle C_r (center at O_r, radius d_c) and outside the circle C_q (center at O_q, radius = semimajor axis of the q th cylinder), the fields described in the q th cylinder coordinates can be expressed in terms of the r th cylinder coordinates. Saermark [17] has shown that the following relation will hold within the above mentioned region:

$$R^{(i)}_{e_o\,m}(c_q,\xi_q)S_{e_o\,m}(c_q,\eta_q)= \sum_{l=0}^{\infty} WE^{q\to r}_{e_o lm}\,\mathrm{Re}^{(i)}_l(c_r,\xi_r)Se_l(c_r,\eta_r) + \sum_{l=1}^{\infty} WO^{q\to r}_{e_o lm}Ro^{(i)}_l(c_r,\xi_r)So_l(c_r,\eta_r) \quad \text{(A1)}$$

Where

$$WE^{q\to r}_{e_o lm}=\frac{\pi(j)^{l-m}}{Ne_l(c_r)}\sum_{i=0}^{\infty}{}'\sum_{p=0}^{\infty}{}'(-j)^{i+p}D^{m}_{e_o i}(c_q)D^{l}_{e\,p}(c_r)X^{q\to r}_{e_o ip} \quad \text{(A2)}$$

$$WO^{q\to r}_{e_o lm}=\mp\frac{\pi(j)^{l-m}}{No_l(c_r)}\sum_{i=0}^{\infty}{}'\sum_{p=0}^{\infty}{}'(-j)^{i+p}D^{m}_{e_o i}(c_q)D^{l}_{o\,p}(c_r)Y^{q\to r}_{e_o ip} \quad \text{(A3)}$$

$$X^{q\to r}_{e_o ip}=J_{p-i}(kd_c)\begin{bmatrix}\cos\\ \sin\end{bmatrix}\psi^{-}+(-1)^i J_{p+i}(kd_c)\begin{bmatrix}\cos\\ \sin\end{bmatrix}\psi^{+} \quad \text{(A4)}$$

$$Y^{q\to r}_{e_o ip}=J_{p-i}(kd_c)\begin{bmatrix}\sin\\ \cos\end{bmatrix}\psi^{-}-(-1)^i J_{p+i}(kd_c)\begin{bmatrix}\sin\\ \cos\end{bmatrix}\psi^{+} \quad \text{(A5)}$$

$$\psi^{+}=i\psi_{qr}+p\psi_{rq}\quad,$$
$$\psi^{-}=i\psi_{qr}-p\psi_{rq}$$

and d_c is the distance between the center lines of the q th cylinder and the r th cylinder, ψ_{rq} is the angle between the $x-$axes of the r th and the q th cylinders measured from the r th cylinder's $x-$axis and $J_p(u)$ is the Bessel function of order p and argument u. The prime over the summation sign $\sum'$ indicates that the sum is over only even or odd values of i (p) depending on whether m (l) is even or odd. The coefficients D_{ei}^{n} and D_{oi}^{m} are the Fourier series coefficients of the Mathieu functions [15].

References:

[1] Z. Zaharis, On the Design of Mobile Base Station Antenna Arrays by Combining an Iterative Perturbation Process and the Orthogonal Method, WSEAS Trans. on Communications, Volume 6, Issue 1, pp. 1-8, 2007.

[2] E. Hamiti, L. Ahma, and A. Sebak, Computer Aided Design of U-Shaped Rectangular Patch Microstrip Antenna for Base Station Antennas of 900 MHz System, WSEAS Trans on Communications, Vol. 5, pp. 961-969, 2006.

[3] Z. Zaharis, D. Kampitaki, A. Papastergiou, A. Hatzigaidas, P. Lazaridis, M. Spasos, Optimal Design of a Linear Antenna Array using Particle Swarm Optimization, WSEAS Trans. on Communications, Volume 5, Issue 12, pp. 2142-2147, 2006.

[4] S. Silver and W. K. Saunders, The radiation from a transverse rectangular slot in a circular cylinder, J. appl. Phys., Vol. 21, 1950, pp. 153-158.

[5] L. I. Bailin, The radiation field produced by a slot in a large circular cylinder, IRE Trans, Vol. 3, 1955, pp. 128-137.

[6] J. Y. Wong, Radiation patterns of slotted elliptic cylinder antennas, IRE Trans .,Vol. 3, 1955, pp. 200-203.

[7] R. A. Hurd, Radiation pattern of a dielectric-coated axially slotted cylinder, Can. J. Phys., Vol.34, 1956, pp. 638-642.

[8] J. R. Wait, and W. Mientka, Slotted-cylinder antenna with a dielectric coating, J. Res. Nat. Bur. Stand, Vol. 58, 1957, pp. 287-296.

[9] W. F. Crosswell, G. C. Westrick, and C.M. Knop, Computations of the aperture admittance of an axial slot on a dielectric coated cylinder, IEEE Trans., Vol. 20, 1972, pp. 89-92.

[10] J. H. Richmond, Axial slot antenna on dielectric-coated elliptic cylinder, IEEE Trans. Ant. Propag., Vol. 37, 1989, pp. 1235-1341.

[11] H. Ragheb, A. Sebak, and L. Shafai, Radiation by axial slots on a dielectric-coated non-confocal conducting elliptic cylinder, IEE Proc. Microw. Ant. Propag., Vol. 143, 1996, pp. 124-130.

[12] M. Hussein, and A. Hamid, Radiation characteristics of N axially slotted antenna on a lossy dielectric-coated elliptic cylinder, Can. J. Phys., Vol. 82, 2004, pp. 141-149.

[13] M. Hussein, and A. Hamid, Exact radiation for slotted circular or elliptical antenna coated by a concentric isorefractive metamaterials, Int. J. Appl. Electroma. Mech., Vol. 26, 2007, pp. 101-111.

[14] A. Tadjalli, A. R. Sebak, and T. A. Denidni, Resonance Frequencies and Far Field Patterns of Elliptical Dielectric Resonator Antenna: Analytical Approach, *Progress In Electromagnetics Research*, PIER 64, 2006, pp. 81-98.

[15] F. A. Alhargan, A complete method for the computations of Mathieu characteristic numbers of integer orders, *SIAM Rev.* 38, 2, 1996, pp. 239–255.

[16] P.M. Morse and H. Feshbach, "Methods of theoretical Physics", Vols. I and II, McGraw-Hill, New York, 1953.

[17] K. Saermark, "A note on addition theorems of Mathieu functions," MZ. Math. Phys., vol. 10, 1959, pp. 426-428.